

Rhodium(I)-catalyzed polymerization of fluorenylacetylenes*

P. Mastrorilli,^a C. F. Nobile,^a G. P. Suranna,^{a*} R. Grisorio,^a
D. Acierno,^b and E. Amendola^c

^aDepartment of Water Engineering and Chemistry, Chemistry Section,
Polytechnic of Bari, via Orabona, 4 I-70125 Bari, Italy
E-mail: surannag@poliba.it

^bDepartment of Materials and Production Engineering (DIMP),
University of Naples Federico II, Naples, Italy

^cInstitute of Composite and Biomedical Materials (IMCB), Italy's CNR, p.le Tecchio 80,
I-80125 Naples, Italy.

The synthesis and characterization of poly(monofluorenylacetylenes) obtained by polymerization of 2-ethynyl-9,9-bis[(*S*)-3,7-dimethyl-octyl]fluorene and 2-ethynyl-9,9-bis[(*S*)-2-methylbutyl]fluorene are described. The effect of the structure of the alkyl chain at the C(9) position of fluorene on the properties of the materials was studied by differential scanning calorimetry, thermogravimetric analysis, X-ray diffraction analysis, UV/Vis spectroscopy, photoluminescence, and circular dichroism. Polymerization of chiral 2-ethynylterfluorene functionalized with (*S*)-2-methylbutylalkyl chains was studied. The resulting polymer exhibits high thermal stability; its emission spectrum occurs in the violet-blue region and shows no significant red shift on passing from a solution to the solid state.

Key words: polyacetylenes, rhodium(I) catalysis, oligofluorenes.

Polyacetylenes are considered to be prototypes of π -conjugated organic materials.¹ A number of properties of these macromolecules have now been investigated.^{2–4} Poly(acetylenes) are generally obtained by transition metal-catalyzed polyaddition of terminal and internal acetylenes. The choice of the catalytic system depends on the monomer structure. It is well known that rhodium(I)-based catalysts are active only toward terminal acetylenes, while Mo^V and W^{VI} systems can also promote polymerization of internal acetylenes. The discovery of efficient and stereospecific Rh^I catalysts for arylacetylene polymerization⁵ has stimulated studies aimed at elucidating the relationship between the properties of poly(arylacetylenes) and the backbone structure.⁶ It has been reported⁷ that an appropriate choice of a Rh^I catalyst produces highly stereoregular cis-transoid backbone configuration, which underlies not only an important secondary helical structure but also a quaternary columnar aggregation.⁷ Moreover, it is known⁸ that polyacetylenes obtained by Rh^I-catalyzed polymerization of chiral functionalized acetylenes may acquire a helical conformation with one predominant helix sense.

* Based on the report presented at the International Conference "Modern Trends in Organoelement and Polymer Chemistry" dedicated to the 50th anniversary of the A. N. Nesmeyanov Institute of Organoelement Compounds of the Russian Academy of Sciences (Moscow, May 30–June 4, 2004).

The emission properties of polyacetylenes may be due to the polyene backbone, the pendant groups, or both.⁹ While several pendant groups with potential emission properties like carbazole,¹⁰ pyrenes,¹¹ and substituted silanols¹² have been synthesized, incorporation of monodisperse π -conjugated oligomers as pendant moieties in a suitable rigid polymeric backbone (such as polyacetylene with bulky pendant groups) has been overlooked. This approach may, in principle, combine a high-molecular-weight material (necessary for solution processability) with well-defined optical properties of oligomers. The only relevant example is polyacetylene with the oligo(phenylenevinylene) pendant groups.¹³

The aim of our research is to synthesize oligofluorene-functionalized polyacetylenes in order to study the influence of the secondary structure of the backbone on the spatial disposition of the fluorene luminophores. Therefore, we have prepared and polymerized two fluorenylacetylene monomers substituted by the chiral (*S*)-2-methylbutyl and (*S*)-3,7-dimethyloctyl chains in the C(9) position. The polymers were investigated by IR and UV/Vis spectroscopy, differential scanning calorimetry, thermogravimetric and X-ray diffraction analyses, circular dichroism, and photoluminescence. The presence of chiral moieties allowed us to investigate the secondary helical arrangement of the polyene backbone by circular dichroism (CD) measurements. As an extension of the

model systems to materials potentially applicable to thin film devices, the polymer obtained by Rh^{I} -catalyzed polymerization of terfluorenylacetylene functionalized by chiral C_5 -alkyl groups was studied for comparison.

Results and Discussion

The monomers, 2-ethynyl-(9,9-bis[(*S*)-3,7-dimethyloctyl]fluorene (**C10FA**) and 2-ethynyl-9,9-bis[(*S*)-2-methylbutyl]fluorene (**C5FA**), containing monofluorene units, are shown in Fig. 1. The different alkyl chains at the C(9) position of fluorene were chosen in order to investigate the influence of steric hindrance on the conformational properties of the macromolecules obtained by Rh^{I} -catalyzed polymerization. The presence of chiral centers in the alkyl chains was meant for investigation of the secondary helical arrangement of the functionalized polyene backbone.¹⁴

The terfluorene-based monomer (**TerFA**) was synthesized as the first step toward the potential extension of the scope of the reaction to more extended fluorene oligomers as emitting materials.

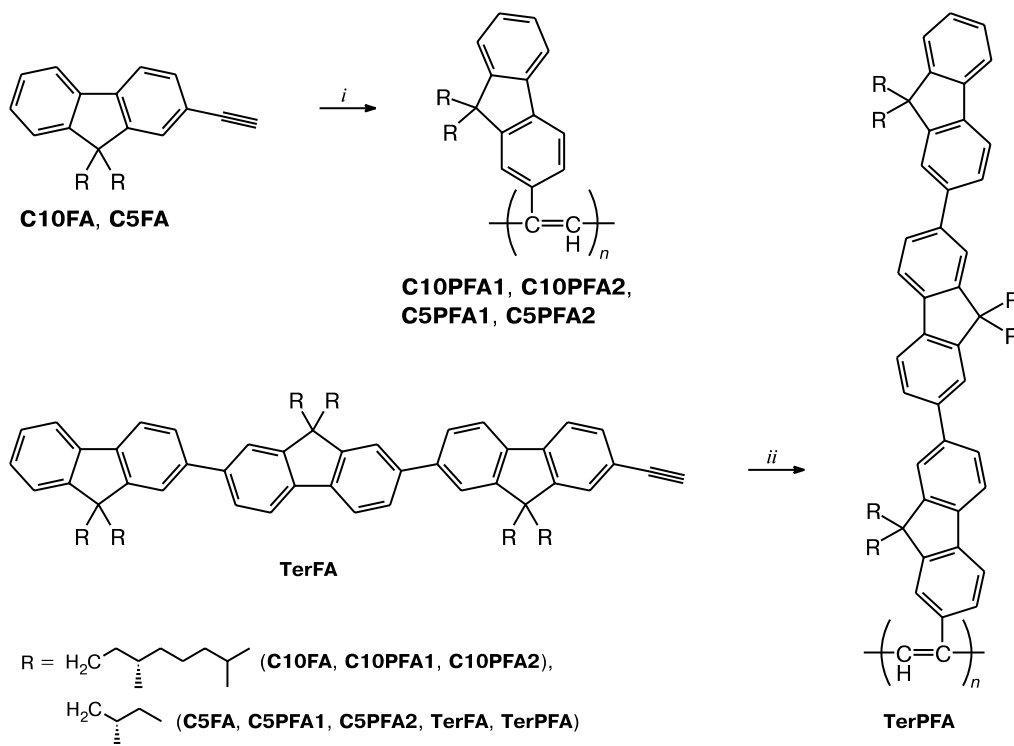
Polymerization. 2-Ethynyl-(9,9-bis[(*S*)-3,7-dimethyloctyl]fluorene (**C10FA**) and 2-ethynyl-9,9-bis[(*S*)-2-methylbutyl]fluorene (**C5FA**) were polymerized in the

presence of $[(\text{nbd})\text{RhCl}]_2$ in Et_3N or $\text{THF}-\text{Et}_3\text{N}$ to yield polymers **C10PFA1,2** and **C5PFA1,2**.¹⁵

The catalytic system was chosen as to ensure a high *cis*-stereoregularity of the polymer backbone.⁵ After the reaction, the products were precipitated with methanol and repeatedly washed with ethanol to eliminate traces of oligomers and cyclotrimers. In neat Et_3N , polymerization of C_{10} -functionalized **C10FA** afforded the soluble **C10PFA1** polymer with an M_n of 47000 Da, while C_5 -functionalized monomer (**C5FA**) was converted into an insoluble material (**C5PFA1**). In order to obtain soluble polyacetylenes, we carried out polymerization in the $\text{Et}_3\text{N}-\text{THF}$ mixed solvent; this gave polymers **C10PFA2** and **C5PFA2**. Polymerization of **TerFA** carried out under conditions that provided soluble polymers in the case of **C10FA** and **C5FA** resulted unfortunately in the formation of an insoluble material. Polymerization of **TerFA** was, therefore, carried out in toluene, at a lower monomer/catalyst ratio, and at higher dilution. This gave a polymer soluble in chloroform and toluene, although the polydispersity of this material was higher (4.0). The reaction conditions and the main properties of the products are summarized in Table 1.

The polymerization products were studied by IR spectroscopy. The spectra invariably showed disappearance of

Scheme 1



Reagents: *i.* $[\text{Rh}(\text{nbd})\text{Cl}]_2$ (nbd is norbornadiene), Et_3N (for **C10PFA1** and **C5PFA1**), $\text{THF}-\text{Et}_3\text{N}$ (for **C10PFA2** and **C5PFA2**); *ii.* $[\text{Rh}(\text{nbd})\text{Cl}]_2$, toluene- Et_3N .

Table 1. Polymerization of **C10FA** and **C5FA**

Monomer	Polymer	Solvent	Yield (%)	M_n	M_w/M_n	Color
C10FA ^a	C10PFA1	Et ₃ N	56	47000	2.2	Brown
C10FA ^a	C10PFA2	THF—Et ₃ N	61	70000	1.9	Orange
C5FA ^a	C5PFA1	Et ₃ N	50	—	—	Brown
C5FA ^a	C5PFA2	THF—Et ₃ N	56	100000	1.9	Brown
TerFA ^b	TerPFA	Toluene—Et ₃ N	79	6000	4.0	Brown

^a [Monomer]/[Cat] = 100; time = 24 h.^b [Monomer]/[Cat] = 10; time = 24 h.

the typical stretching bands of terminal acetylenes. The ¹H NMR spectra of **C10PFA2** and **C5PFA2** in CD₂Cl₂ or CDCl₃ did not help in assessing the polymer stereoregularity, as they exhibited only broad humps in the region of aromatic protons.

Thermal and structural properties. According to TGA measurements (Table 2), all of the polymers are stable up to 290 °C. This thermal stability is the result of an efficient wrapping of bulky pendant groups around the conjugated double bonds. The *cis*-to-*trans* isomerization of the polyene backbone¹⁶ is revealed by the presence of an exothermic peak observed for samples **C10PFA1**, **C10PFA2**, **C5PFA1**, and **C5PFA2** close to the onset of decomposition. Notably, in the case of **C10PFA1** and **C10PFA2**, an endothermic peak was observed at 170 °C, while no such peaks could be detected for **C5PFA1** and **C5PFA2**. This difference in the thermal behaviors could be related to the dimension of the alkyl chains in the two polymers, in particular, the bulky C₁₀ pendants linked to the polyene backbones in **C10PFA1** and **C10PFA2** are subject to easier segmental movements, and this may account for the temperature transition observed. No clear DSC transitions were found for **TerPFA**, presumably due to the rigid structure of the polymer. The X-ray diffraction data provided an insight into the molecular packing of the polymers. Both **C10PFA1** and **C10PFA2** show broad Bragg reflections at a high 2θ values (corresponding to a layer spacing of 4.60 Å) and a relatively sharp reflection at low 2θ values (corresponding to a layer spacing of 19.9 Å). The samples **C5PFA1** and **C5PFA2** show a slightly more

structured pattern. Evidently, polymerization in Et₃N results in a higher aggregation of the polymer chain. However, the broadness of the peaks points to a very low degree of crystallinity of the polymers synthesized. The reflections at low 2θ values can be attributed to the distances between the polyene backbones.¹⁷ The shorter alkyl groups in **C5PFA1** and **C5PFA2** lead to a bilayer arrangement with shorter interchain distances (17.7 Å and 16.4 Å) compared to those in **C10PFA1** and **C10PFA2** (19.9 Å). The peaks at 4.60 Å and 4.46 Å are determined by the interplane distances between the fluorene systems arranged parallel to each other. The terfluorene-based polymer (**TerPFA**) is entirely amorphous because of the great bulk of the pendant group, which prevents a regular three-dimensional organization.

UV/Vis and photoluminescence properties. The UV/Vis absorption spectra of **C10PFA2** and **C5PFA2** in solution (CHCl₃) and the spectrum of **TerPFA** in solution and in thin film (obtained by spin coating from a solution in CHCl₃ with a concentration of 1 mg mL⁻¹) are shown in Fig. 1. The absorption spectra of polymers **C10PFA2** and **C5PFA2** in solutions are very similar (see Fig. 1, a), due to the similarity of their primary structure (λ_{max} = 320, 290 nm). These bands are due to the π—π* transitions of the fluorene units. The peaks at 458 and 445 nm, respectively, in the spectra of **C10PFA2** and **C5PFA2** are ascribable to the π—π* transitions of the polyene backbones. These bands are red-shifted with respect to those of analogous polyenes (for instance, the corresponding absorption band in the spectrum of poly(phenylacetylene) occurs at about 400 nm), thus pointing out a longer conju-

Table 2. TGA and DSC data for poly(fluorenylacetylenes)

Polymer	$T_{\max}/^{\circ}\text{C}$ ^a		$T_{\text{dec}}/^{\circ}\text{C}$ ^b
	<i>endo</i>	<i>exo</i>	
C10PFA1	170	286	300
C10PFA2	170	288	290
C5PFA1	—	297	300
C5PFA2	—	299	300
TerPFA	—	—	340

^a *endo* is an endothermic peak, *exo* is an exothermic peak.^b Decomposition (for 5% weight loss).**Table 3.** X-Ray diffraction reflections of poly(fluorenylacetylenes)

Sample	Reflections/Å	
	strong and medium	weak and broadened
C10PFA1	19.9 (s)	4.60
C10PFA2	19.9 (s)	4.60
C5PFA1	17.7 (br.m)	4.46, 6.08, 7.82
C5PFA2	16.4 (br.m)	—

Note. **TerPFA** is amorphous.

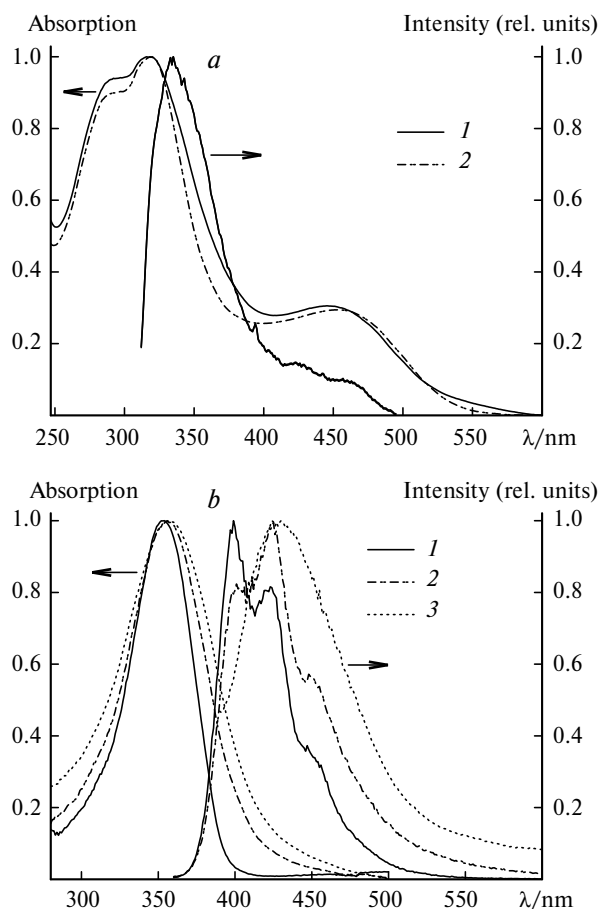


Fig. 1. (a) UV/Vis and photoluminescence spectra of **C10PFA2** (1) and **C5PFA2** (2) in CHCl_3 . (b) UV/Vis and photoluminescent spectra of **TerFA** in CHCl_3 (1) and **TerPFA** in CHCl_3 (2) and as a thin film (3).

gation chain in the polyene backbone. The planarization is presumably a consequence of the twisting of the fluorene groups orthogonally with respect to the backbone plane caused by the steric repulsion between the bulky pendant groups, which has already been observed in similar systems.¹⁸ The red shift (13 nm) of the backbone absorption band of **C10PFA2** with respect to that of **C5PFA2** is attributable to a more planar conformation of the former.

The photoluminescence (PL) spectra of **C10PFA2** and **C5PFA2** recorded with $\lambda_{\text{ex}} = 290$ nm show a maximum at 337 nm. No signal was detected by recording the PL spectra at $\lambda_{\text{ex}} = 450$ nm, which confirms the weak emitting ability of polyacetylenes.⁴

Figure 1, b shows the absorption spectra of **TerPFA** in solution and in the solid state. A solution of the **TerFA** monomer exhibits a maximum at 353 nm, corresponding to the $\pi-\pi^*$ transition of the terfluorene unit. A solution of **TerPFA** in CHCl_3 shows an absorption band slightly red-shifted with respect to that of the monomer (356 nm) and a tail at longer wavelengths attributable to the $\pi-\pi^*$

transition of the polyene backbone. The appearance of this band as a tail can be a consequence of the much higher extinction coefficient of terfluorene compared to that of the polyacetylene backbone leading to a minor contribution of the $\pi-\pi^*$ absorption of the polyene backbone to the overall absorption spectrum of **TerPFA**. A spin-coated film of the polymer shows an absorption curve represented by a broad band centered at 358 nm.

The fluorescence spectra of **TerPFA** ($\lambda_{\text{ex}} = 350$ nm) in solution show a vibronic fine structure typical of terluorene units (the absolute maximum occurs at 425 nm). In the solid state, the emission band falling in the violet-blue region ($\lambda_{\text{max}} = 430$ nm) exhibits no vibronic fine structure.

Chiroptical properties. The chiral centers in the side chains at the C(9) position in the monomers can be used for probing the helical arrangement of the functionalized polyene backbones. In fact, if an excess in one of the screw senses of the helix is induced, a Cotton effect would be observed in the circular dichroism (CD) spectra of the macromolecules.¹⁹ The CD spectra of **C10PFA2** and **C5PFA2** (Fig. 2, a) in CHCl_3 recorded at room temperature showed a pronounced Cotton effect in the region of the polyene backbone absorption.

In the case of **C5PFA2**, the Cotton effect is more pronounced; the difference in the CD response intensity

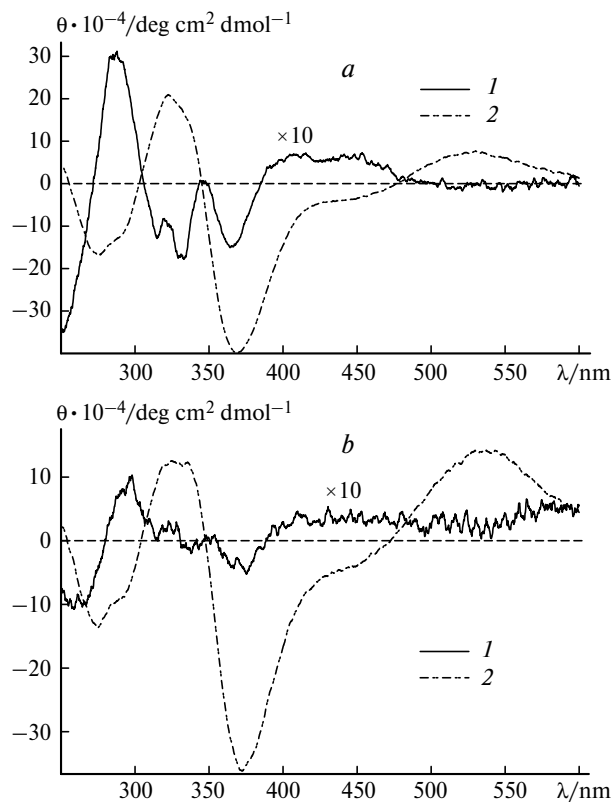


Fig. 2. (a) Circular dichroism spectra of **C10PFA2** (1) and **C10PFA2** (2) in CHCl_3 . (b) Circular dichroism spectra of **C10PFA2** (1) and **C5PFA2** (2) in $\text{MeOH}-\text{CHCl}_3 = 90 : 10$.

between the two polymers may be due either to the close positions of the polyene backbone and the chiral center or to the steric hindrance created by the pendant groups. The considerably lower Cotton effect observed for **C10PFA2** can be ascribed to the influence of the (*S*)-3,7-dimethyloctyl chains which, as confirmed by the UV/Vis spectra, may be responsible for stabilization of the planar polyene conformation.²⁰ The opposite signs of the predominant chiroptical properties of the two polymers can be regarded as a consequence of the opposite screw sense of the two helices induced by the different alkyl chains. The weak Cotton effect observed for **C10PFA2** was completely lost when the spectrum was recorded in a methanol–chloroform (90 : 10) mixture, because of the poor solvating properties of methanol favoring planarization of the backbone. Interestingly, the Cotton effect is retained for **C5PFA2** in a methanol–chloroform solution (see Fig. 2, *b*). No chiroptical properties either in solution or in the solid state were observed for **TerPFA** notwithstanding the presence of the (*S*)-2-methylbutyl groups (which ensure the good CD response observed for **C5PFA2**). The size of the terfluorene moiety, which destabilizes any helical secondary structure, may account for the lack of induction of any preferential screw sense in the polyene backbone.

Thus, we described Rh^I-catalyzed polymerization of fluorenylacetylenes. Terminal acetylenes were functionalized by 2-ethynyl-(9,9-bis[(*S*)-3,7-dimethyloctyl]fluorene and 2-ethynyl-9,9-bis[(*S*)-2-methylbutyl]fluorene groups and polymerized under various conditions. High thermal stability of the polymers was proven by DSC-TGA measurements. X-Ray diffraction data point to a bilayer arrangement of the polymer chain. A helical conformation of the polyene backbone for the two polymers was evidenced by circular dichroism investigations.

A synthetic route was devised for inserting a terminal acetylene into a chiral C₅-functionalized terfluorene moiety. Analysis of the polymer confirmed the thermal stability observed for the model systems. The UV/Vis features of the monomer and the polymer correspond to those typical of a molecularly dissolved terfluorene systems. The emitting properties of a spin-coated film of the terfluorene-based polymer follow those found in solution. Moreover, the emission spectra occur in the violet-blue region and do not show any substantial red shift on passing from solution to the solid state.

Experimental

All operations were carried out in inert atmosphere (nitrogen) using common Schlenk techniques and freshly distilled solvents. UV/Vis spectra were recorded on a Kontron Uvikon 942 spectrophotometer; fluorescence spectra were obtained on a Varian Cary Eclipse spectrofluorimeter. FT-IR spectra were recorded on a Bruker Vector 22 spectrometer. CD spectra were

recorded with a Jasco J-810 spectropolarimeter. Mass spectra were run on an HP 5973 instrument. GPC analyses were carried out on an HP 1050 instrument equipped with a PL-gel 5 mm mixed-D column (300 mm×7.5 mm). GPC analysis was carried out with THF solutions, which were eluted at 25 °C at a flow rate of 1 mL min⁻¹ and analyzed using a multiple wave detector ($\lambda = 320$ and 350 nm). The molecular weights and molecular weight distributions are given relative to polystyrene standards. Thermogravimetric analyses were carried out with a TA Instruments 2590 thermobalance; differential scanning calorimetry was done on a TA Instruments 2920 calorimeter. Both thermal analyses were carried out under nitrogen with a heating rate of 10 deg min⁻¹. X-Ray diffraction measurements were carried out with imaging plates located at a distance of 10 cm from the substances, a current of 20 mA, and a voltage of 40 kV (CuK α radiation, Ni-filter). The monomers **C10FA**, **C5FA**, and **TerFA** were prepared as described previously.²¹

Poly{9,9-bis[(*S*)-3,7-dimethyloctyl]fluorene-2-ylacetylene} (C10PFA1**). A 50-mL round-bottom flask was charged with [Rh(nbd)Cl]₂ (3.46 mg, 0.75·10⁻² mmol) and Et₃N (1.7 mL), and the solution was stirred for 15 min. Subsequently, a solution of **C10FA** (0.353 g, 0.75 mmol) in Et₃N (3.0 mL) was added. The color of the solution turned instantly from light-yellow to dark-brown. The reaction mixture was stirred for 24 h. The polymer was precipitated by dropwise addition of the reaction mixture to a beaker containing 200 mL of methanol kept under stirring followed by filtering of the resulting suspension. The orange solid was washed with ethanol and dried under vacuum (56%). IR (KBr), ν /cm⁻¹: 3056, 2962, 2868, 1458, 1259, 1091, 1018, 834, 798, 740.**

Poly{9,9-bis[(*S*)-3,7-dimethyloctyl]fluorene-2-ylacetylene} (C10PFA2**). A 50-mL round-bottom flask was charged with [Rh(nbd)Cl]₂ (2.44 mg, 0.53·10⁻² mmol) and Et₃N (1.5 mL), and the solution was stirred for 15 min. Subsequently, a solution of **C10FA** (0.250 g, 0.53 mmol) in THF (2.0 mL) was added. The color of the solution turned instantly from light-yellow to dark-brown. The reaction mixture was stirred for 24 h. The polymer was precipitated by dropwise addition of the reaction mixture to a beaker containing 200 mL of methanol kept under stirring followed by filtering of the resulting suspension. The orange solid was washed with ethanol and dried under vacuum (61%). IR (KBr), ν /cm⁻¹: 3056, 2976, 2868, 1458, 1259, 1091, 1018, 798, 740.**

Poly{bis[(*S*)-2-methylbutyl]fluorene-2-ylacetylene} (C5PFA1**). The reaction was carried out under the same conditions as that for **C10PFA1** (**C5FA**, 0.290 g, 0.87 mmol; [Rh(nbd)Cl]₂, 4.00 mg, 0.87·10⁻² mmol; Et₃N, 5.5 mL). This gave a brown solid (50%). IR (KBr), ν /cm⁻¹: 3056, 2962, 2868, 1458, 1369, 1254, 1091, 1002, 834, 740.**

Poly{9,9-bis[(*S*)-2-methylbutyl]fluorene-2-ylacetylene} (C5PFA2**). The reaction was carried out under the same conditions as that for **C10PFA2** (**C5FA**, 0.200 g, 0.61 mmol; [Rh(nbd)Cl]₂, 2.81 mg, 0.61·10⁻² mmol; Et₃N, 1.5 mL; THF, 2.3 mL). This gave a brown solid (56%). IR (KBr), ν /cm⁻¹: 3056, 2962, 2868, 1458, 1369, 1091, 1002, 834, 740.**

Poly{9,9,9',9',9'',9''-hexakis[(*S*)-2-methylbutyl]-7,2';7',2''-terfluorene-2-ylacetylene} (TerPFA**). A 50-mL round-bottom flask was charged with [Rh(nbd)Cl]₂ (5.50 mg, 0.012 mmol) and Et₃N (2.0 mL) and the solution was stirred for 15 minutes. Subsequently, a solution of **TerFA** (0.110 g, 0.12 mmol) in toluene (40 mL) was added. The color turned**

from light-yellow to dark-brown. The reaction mixture was stirred for 24 h and then was added dropwise to a beaker containing 200 mL of methanol kept under stirring. The suspension was filtered and the solid residue was washed with ethanol to afford the product as a brown powder (79%). IR (KBr), ν/cm^{-1} : 3058, 2957, 2870, 1460, 1376, 1261, 1097, 1020, 814, 740.

This research was financed by Italian MIUR (FIRB project MICROPOLYS). The authors gratefully acknowledge Dr. Antonino Rizzuti and Prof. Pio Iannelli for helpful discussions.

References

1. H. Shirakawa, E. J. Louis, A. G. MacDiarmid, C. K. Chiang, and A. J. Heeger, *J. Chem. Soc., Chem. Comm.*, 1977, 578.
2. E. T. Kang, K. G. Neoh, T. M. Masuda, T. Higashimura, and M. Yamamoto, *Polymer*, 1989, **30**, 1328.
3. J. Le Moigne, A. Hilberer, and C. Strazielle, *Macromolecules*, 1992, **25**, 6705.
4. C. W. Lee, K. S. Wong, W. Y. Lam, and B. Z. Tang, *Chem. Phys. Lett.*, 1999, **307**, 64.
5. Y. Kishimoto, P. Eckerle, T. Miyatake, M. Kainosho, A. Ono, T. Ikariya, and R. Noyori, *J. Am. Chem. Soc.*, 1999, **121**, 12035.
6. M. Kozuha, T. Sone, Y. Sadayiro, M. Tabata, and T. Enoto, *Macromol. Chem. Phys.*, 2002, **203**, 66.
7. Y. Mawatari, M. Tabata, T. Sone, K. Ito, and Y. Sadahiro, *Macromolecules*, 2001, **34**, 3776.
8. T. Nakano and Y. Okamoto, *Chem. Rev.*, 2001, **101**, 4013.
9. J. W. Y. Lam and B. Z. Thang, *J. Polym. Sci., Part A: Polym. Chem.*, 2003, **41**, 2607.
10. F. Sanda, T. Nakai, N. Kobayashi, and T. Masuda, *Macromolecules*, 2004, **37**, 2703.
11. E. Rivera, M. Belletete, X. X. Zhu, G. Durocher, and R. Giasson, *Polymer*, 2002, **43**, 5059.
12. J. Chen, Z. Xie, J. Lam, C. Law, and B. Z. Tang, *Macromolecules*, 2003, **36**, 1108.
13. A. P. H. J. Shennings, M. Fransen, J. K. J. van Duren, P. A. van Hal, R. A. J. Janssen, and E. W. Meijer, *Macromol. Rapid Commun.*, 2002, **23**, 271.
14. G. Gao, F. Sanda, and T. Masuda, *Macromolecules*, 2003, **36**, 3932.
15. M. Nakamura, M. Tabata, T. Sone, Y. Mawatari, and A. Miyasaka, *Macromolecules*, 2002, **35**, 2000.
16. V. Percec, J. Rudick, P. Nombel, and W. Buchowicz, *J. Polym. Sci., Part A: Polym. Chem.*, 2002, **40**, 3212.
17. B. Z. Tang, X. Kong, X. Wan, H. Peng, W. Lam, X. Feng, and H. Kwok, *Macromolecules*, 1998, **31**, 2419.
18. S. Lee, B. Jang, and T. Tsutsui, *Macromolecules*, 2001, **35**, 1356.
19. (a) K. Akagi, G. Piao, S. Kaneko, K. Sakamaki, H. Shirakawa, and M. Kyotani, *Science*, 1998, **282**, 1683; (b) K. Shinoara, S. Yasuda, G. Kato, M. Fujita, and H. Shigekawa, *J. Am. Chem. Soc.*, 2001, **123**, 3619.
20. V. Percec, M. Obata, J. G. Rudick, R. B. De, M. Glodde, T. K. Bera, S. N. Magonov, V. S. K. Balagurusamy, and P. A. Heiney, *J. Polym. Sci., Part A: Polym. Chem.*, 2002, **40**, 3509.
21. P. Mastrorilli, C. F. Nobile, R. Grisorio, A. Rizzuti, G. P. Suranna, D. Acierno, E. Amendola, and P. Iannelli, *Macromolecules*, 2004, **37**, 4488.

Received June 24, 2004